

A Fiber Laser Photonic Frequency Synthesizer: Concept, Performance, and Applications

Michael C. Gross, Patrick T. Callahan,
and Michael L. Dennis

We have developed a tunable photonic source of precision frequencies in the RF, microwave, and millimeter-wave regimes. This source is based on a laser that uses stimulated Brillouin scattering in optical fiber as its gain mechanism, lasing on two wavelengths simultaneously. The lasing modes are heterodyned on a photodiode to produce the desired output frequency. These modes can be arbitrarily far apart, allowing very high frequencies to be generated. The lasing lines share a single cavity, so that the dominant noise mechanisms cancel. As a result, the output beat frequency exhibits a narrow linewidth and low phase noise. In this article, we describe the laser and its use as a photonic frequency synthesizer: its stepwise tunability, its potential for higher-frequency operation, its linewidth and noise characteristics, and its applications.

INTRODUCTION

Low-phase-noise microwave oscillators are essential for a number of military and commercial applications, and many of these applications require the output frequencies to be tunable over a broad range. Commercial applications include high-precision frequency or timing references for communications, fiber remoting of antennas for fiber radio,^{1,2} precision clocks, and Global Positioning System (GPS) navigation. Additional commercial applications include master oscillators for RF

and microwave-frequency synthesizers as well as high-precision clocks for test and measurement and for research. An important military application is reference oscillators for coherent RF sensors.³

A number of tunable, high-frequency sources have been demonstrated that are based on the heterodyning of two laser frequencies, either between independent lasers^{4–6} or between two laser modes sharing a common cavity and common gain.^{7–12} In the first approach, all

phase noise and drift from each laser is directly transferred onto the RF signal; therefore, exceptionally stable lasers are required to obtain a narrow linewidth and low phase noise in the RF domain. The second approach eliminates this problem in that the dominant noise processes originate with the laser cavity and thus affect each mode equally; this noise is cancelled out when the two frequencies are differenced. However, most laser gain media are homogeneously broadened, which means that the radiating sites (atoms, ions, or molecules) all experience the same linewidth-broadening mechanisms. As a result of this homogeneity, all the sites can radiate into all the lasing modes in the cavity, and these modes must compete for gain from each of these sites.¹³ For dual-mode (dual-wavelength) operation, this gain competition results in power shifting between the lasing modes, which can severely degrade the amplitude and phase noise of the beat frequency.¹⁴

The dual-wavelength operation of a fiber laser with stimulated Brillouin scattering (SBS) gain^{15,16} avoids both the noise associated with independent lasers and noise due to gain competition between wavelengths in a single cavity. Over the past several years, we have developed an a photonic frequency synthesizer (FPS) based on a laser of this type under support of internal research and development programs within the APL Air and Missile Defense Business Area. We have shown its output frequency to be discretely tunable up to 100 GHz^{17–20} with a linewidth <1 Hz.^{20,21} We have also reported on this laser's phase noise²² and demonstrated a technique for reducing its amplitude noise.²³ Finally, we have used this laser to photonically upconvert data at rates >1 Gb/s onto a 60-GHz carrier and to transmit that carrier wirelessly,^{19,24} as discussed in detail by Nanzer et al. elsewhere in this issue. In this article, we describe this SBS fiber laser in detail, discuss its frequency-tuning capability, and consider possible operation at even higher frequencies (into the terahertz regime).

CONCEPT

A block diagram of the SBS laser is shown in Fig. 1a. The laser construction is extremely simple, consisting only of a pump laser, an optical circulator, and a fiber ring resonator (FRR). The physical basis for the laser's operation is discussed in the following subsections.

Fiber Ring Resonator

The FRR has been extensively developed over the last 25 years,²⁵ primarily for applications in resonant fiber-optic gyroscopes^{26,27} and optical spectrum analyzers.^{28–30} The FRR consists entirely of a coil of optical fiber spliced to two ports of a four-port coupler. As shown in the Fig. 1, ports B and C are connected such

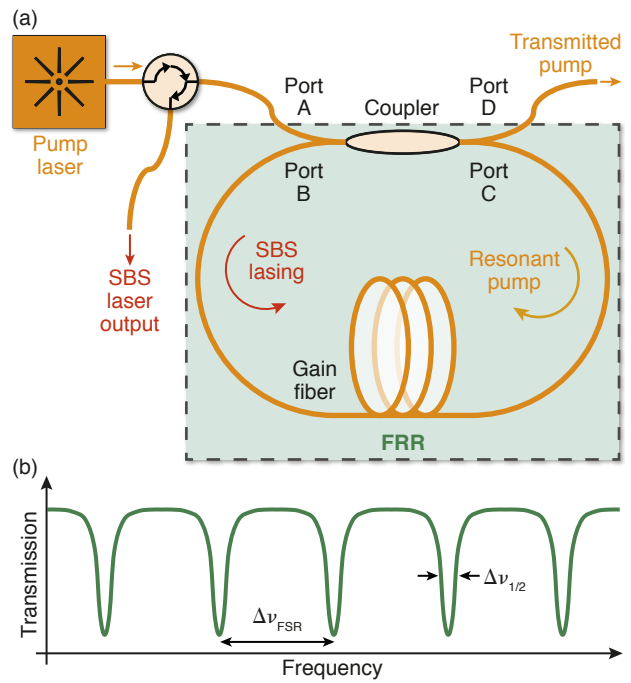


Figure 1. (a) The laser resonator. Note that the SBS propagates oppositely to the pump. (b) Transmission spectrum of the FRR from coupler port A to port D. $\Delta\nu_{1/2}$, full width at half maximum of the transmission resonance; $\Delta\nu_{\text{FSR}}$, free spectral range.

that for light input to port A, some fraction of the light will be coupled over to port C and will thence be transmitted back to port B, the other port at the input end of the coupler. The gain fiber is both single-mode at the desired operating wavelength and polarization maintaining, as is the coupler. The transmission spectrum observed at port D of the coupler consists of periodic minima, as illustrated in Fig. 1b. These minima are located at frequencies ν_N , given by

$$\nu_N = N\Delta\nu_{\text{FSR}} = Nc/nL, \quad (1)$$

where N is an integer, L is the total round-trip length of the FRR, n is the index of refraction, and c is the speed of light in vacuum; the quantity $\Delta\nu_{\text{FSR}} \equiv c/nL$ is referred to as the free spectral range (FSR) of the resonator. These transmission minima result from the fact that, on resonance, all pump light is coupled into the fiber within the FRR. The minima have a width (full width at a transmission halfway between the maximum and minimum values), $\Delta\nu_{1/2}$, given by

$$\Delta\nu_{1/2} = \Delta\nu_{\text{FSR}}/F. \quad (2)$$

The quantity

$$F \equiv \pi \frac{\sqrt[4]{1-\ell}}{1-\sqrt{1-\ell}} \quad (3)$$

is referred to as the finesse of the resonator, where ℓ is the total round-trip loss; for well-constructed designs, the loss is equal to (or only slightly greater than) the fractional output coupling at the coupler. The finesse is related also to the quality factor, Q , of the FRR by the relationship

$$Q = \nu_{\text{opt}}/\Delta\nu_{1/2} = N\Delta\nu_{\text{FSR}}/\Delta\nu_{1/2} = NF, \quad (4)$$

where we have identified the optical frequency ν_{opt} with a resonance of the FRR from Eq. 1. The Q is a generally useful property of resonators, whether optical, electrical, or otherwise, with higher values preferred for low-noise oscillators. For $N \approx 2 \times 10^7$ or higher (appropriate for typical fiber lengths) and $F \approx 20$ –50 (typical for a simple FRR), $Q \approx 10^9$. This is substantially greater than for high-quality microwave resonators. FRRs are commercially available with $F > 3000$ and corresponding $Q > 10^{11}$, far in excess of any standard microwave-frequency resonators.

Stimulated Brillouin Scattering

SBS is a well-known fundamental phenomenon of importance in the propagation of moderate optical powers over single-mode optical fiber for significant distances. The theory of SBS in fibers is extensively developed in chapter 9 of Ref. 31 and in the references contained therein; essential background information is reviewed here. Physically, SBS is the phenomenon of scattering of photons from acoustic phonons in bulk media. In this interaction, both energy and momentum are conserved, so that the following relations are satisfied:

$$\nu' = \nu_0 - \nu_B \quad (5)$$

$$\mathbf{k}' = \mathbf{k}_0 - \mathbf{k}_B \quad (6)$$

Here, the quantities (ν', ν_0, ν_B) and $(\mathbf{k}', \mathbf{k}_0, \mathbf{k}_B)$ are the frequencies and wavevectors, respectively, of the scattered photon, the initial (pump) photon, and the phonon. Phenomenologically, there are two important consequences of Eqs. 5 and 6:

1. The scattered photon is reduced in frequency by an amount ν_B , which is referred to as the Brillouin shift or Stokes shift. The Brillouin shift, ν_B , is a material-dependent parameter; furthermore, it is proportional to the optical frequency of the pump photon and is also weakly dependent on environmental characteristics such as temperature and strain. In standard single-mode silica fiber at a wavelength of 1550 nm, $\nu_B \approx 10$ –12 GHz.
2. The wavevector—i.e., direction of propagation—of the scattered photon is altered substantially. This is due to the fact that, although the energy of an

acoustic phonon is quite small compared with that of a photon, the phonon can carry momentum comparable to or in excess of that of the photon. In a single-mode optical fiber, light can propagate only forward or backward within the fiber; thus, the principal consequence of Eq. 6 is that the scattered photon propagates in the direction *opposite* to that of the pump photon.

The SBS phenomenon therefore results in optical gain at an optical frequency lower than that of the pump, with the difference equal to the Brillouin shift. The homogeneous (intrinsic) linewidth of this gain line is quite narrow, typically ~ 15 MHz.³² Furthermore, this gain can be obtained at *any* optical frequency simply by pumping with photons at a frequency that is higher than that desired by an amount equal to the Brillouin shift. The evolution for the Stokes (Brillouin backscattered) field on propagation along a fiber is given by

$$P_S(z) = P_S(0) \exp(g_B P_{\text{pump}} z / A_{\text{eff}}), \quad (7)$$

where P_S is the power in the Stokes field, z is the distance along the fiber, g_B is the material-dependent peak Brillouin gain coefficient, P_{pump} is the power in the pump, and A_{eff} is the effective area of the mode in the fiber. For standard, single-mode silica fiber and light at 1550 nm, $g_B \approx 5 \times 10^{-11}$ m/W and $A_{\text{eff}} \approx 80 \mu\text{m}^2$. As an example, from Eq. 7 we can calculate that, for a fiber of length $z = 20$ m, a gain of 3 dB results for $P_{\text{pump}} \approx 55.5$ mW. Thus, the Brillouin gain process can be accessed by using pump lasers of modest power, comparable to lasers commonly used in the telecommunications industry.

SBS Fiber Lasers

Because the SBS phenomenon provides optical gain, it can be used to implement a laser. To construct a laser based on SBS, four primary conditions must be met:

1. An optical resonator containing a gain medium must be constructed.
2. A pump source must be provided at a wavelength (frequency) corresponding to a resonance of the resonator.
3. The Brillouin gain line must overlap at least one resonance of the FRR.
4. The pump power must be such that the gain from SBS exceeds the round-trip loss for light propagating around the resonator at the Stokes-shifted wavelength.

These four conditions can be satisfied simultaneously for two separate pump wavelengths. Condition 1 is straightforward; it can be met simply by using the configuration of Fig. 1 with a fiber in the loop that

is sufficiently long to provide gain ($\sim 2\text{--}50$ m is adequate, depending on pump power). In order to satisfy conditions 2–4 for two-wavelength operation, certain relationships among the cavity resonances, pump wavelengths, Brillouin gain bands, and SBS lasing lines are required, as illustrated in Fig. 2. Figure 2a shows the cavity transmission spectrum, as in Fig. 1. Figure 2b shows a single pump wavelength that is modulated to create two pump wavelengths before insertion into the cavity, as illustrated in Fig. 2c. Figure 2d is the spectrum of the two Brillouin gain bands produced by the two pumps. Figure 2e shows the SBS lasing lines that result from each gain band.

Figures 2a–2c illustrate that condition 2 is critical: Typically, the resonance width is on the order of 100–500 kHz. Ideally, the pump laser linewidth should be much less than this. Also, the pump wavelength must track the FRR resonance even as the latter drifts, for example, because of changes in the temperature of the environment of the FRR. Both of these conditions can be met using servo control of the pump source. Figure 2d also illustrates the importance of condition 3: Because lasing will occur only at a resonance of the FRR, there will be no laser if the SBS gain line does not overlap a resonance. Fortunately, the width of an SBS gain line, $\Delta\nu_B$, is comparable to the FSR of an FRR

of typical length (~ 10 MHz for a 20-m cavity), so that this condition is not particularly demanding in practice. Condition 4 is a general requirement for lasing. So long as conditions 3 and 4 are satisfied, lasing will obtain at the frequencies $\nu_{1,\text{out}}$ and $\nu_{2,\text{out}}$, corresponding to the FRR resonances closest to the peak of each respective SBS gain band. If these two lasing lines are heterodyned together on a photodiode, as indicated in Fig. 2f, nonlinear mixing will generate an RF or microwave beat note of frequency f_{out} equal to the optical frequency difference between the two lasing lines. This beat-note frequency is the PFS output, and it will be approximately equal to the difference between the two pumps. We use the word “approximately” because the optical mode frequencies are determined by the narrow cavity resonances rather than the broad gain bands. As a result, the system will suppress any noise on the difference between the pump frequencies, as will be quantified below.

The essential conditions listed above have been understood for some time; the earliest demonstration of an SBS fiber laser was made in 1976.^{33–35} Subsequently, it was recognized that this approach offered some potential for implementation of a low-noise, narrow-linewidth laser.^{36,37} This led to the development of laser gyroscopes based on SBS fiber ring lasers.^{38–44} The

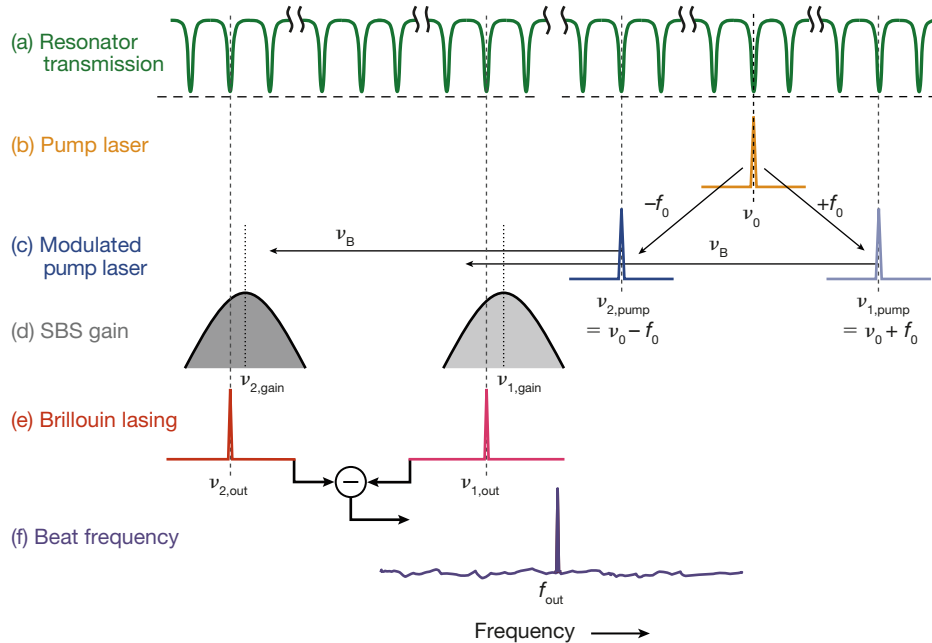


Figure 2. Relationships in optical frequency among the principal physical processes in the photonic frequency synthesizer (PFS). (a) Cavity transmission (green). (b) Initial pump laser (orange). (c) Pump frequencies for two-wavelength operation (blue) obtained by amplitude modulating the initial pump. (d) SBS gain bands (gray). (e) SBS lasing lines (red). (f) Beat note in the RF domain generated by mixing the SBS lasing lines (purple). ν_0 , pump-laser frequency; f_0 , microwave drive frequency; $\nu_{1,\text{pump}}$ and $\nu_{2,\text{pump}}$, higher and lower pump frequencies; ν_B , Brillouin shift; $\nu_{1,\text{gain}}$ and $\nu_{2,\text{gain}}$, frequencies of peak gain for higher and lower gain bands; $\nu_{1,\text{out}}$ and $\nu_{2,\text{out}}$, higher and lower lasing frequencies; f_{out} , beat-note frequency.

success of the Brillouin laser gyroscope depends critically on rejection of common-mode technical noise. Common-mode rejection occurs when two lasing modes share a single cavity; any thermal drift or acoustic vibration will be common to the two modes. In our two-mode laser, this noise will be canceled, to first order, when the two lines are differenced on the photodiode.¹⁸ As a result, the beat-frequency noise will be far lower than the cavity noise.

A key advantage of the dual-wavelength SBS laser, as compared with alternative dual-wavelength-laser techniques for generating high-frequency RF and microwave signals,¹⁰ is that the gain for the two modes is independent: Each mode obtains gain exclusively

from its respective SBS gain band. There is thus no gain competition between the two lasing modes and therefore no competition-induced phase or amplitude noise. Note, however, that the SBS gain itself is homogeneously broadened. This fact helps to ensure that only a single lasing mode—the one with the highest net gain—operates on each gain band, minimizing mode hopping and amplitude noise on each mode.

EXPERIMENTAL SETUP

Figure 3 illustrates the complete PFS, which consists of the SBS laser, its pump subsystem, the heterodyning photodiode, control hardware, and ancillary optical components. The continuous-wave laser provides a single optical tone in the telecommunications band (wavelength $\lambda_0 \approx 1550$ nm, optical frequency $\nu_0 \approx 193$ THz) with a linewidth of <10 kHz; this corresponds to Fig. 2b. The amplitude modulator (an integrated-optic Mach–Zehnder interferometer on lithium niobate⁴⁵) is biased at a null and is driven by the RF oscillator at frequency f_0 (equal to half of the desired output frequency), generating sidebands at $\nu_0 \pm f_0$, which dominate over the original optical carrier tone, as illustrated in Fig. 2c. The oscillator frequency is selected so that both $\nu_0 + f_0$ and $\nu_0 - f_0$ are resonant with the FRR, i.e., such that $2f_0 = N\Delta\nu_{\text{FSR}}$, where N is an integer. The phase modulator is used in one of the servo loops that stabilize the system. The erbium-doped fiber amplifier ensures that the optical power suffices for the SBS laser

to reach threshold. The optical circulator couples the pump lines into the cavity.

The FRR consists of a 20% coupler, a piezoelectric fiber stretcher, and a coil of fiber; all intracavity components and all the components in the pump path are polarization maintaining. The total length of the cavity is ~ 20 m, yielding an FSR of ~ 10 MHz and a resonance width of ~ 500 kHz. When the two pump tones are aligned with the resonances of the FRR, as in Fig. 2c, pump power builds up in the cavity and each produces a Stokes-shifted SBS gain band as shown in Fig. 2d.³⁵ The cavity FSR is less than the Brillouin gain bandwidth, so that at least one cavity resonance will overlap the SBS gain band and lasing will result for each gain band at the cavity resonance with the highest gain. For the fiber used in these experiments, we measured the peak shift and full width at half maximum of the gain band to be 10.868 GHz and 14.6 MHz, respectively, at room temperature. The fiber stretcher allows a small amount of FSR tuning, but it was held fixed during the experiments described here.

Finally, the two lasing lines are coupled out of the cavity and are separated from the pumps by the circulator. The lasing lines are then mixed on a photodiode, producing the PFS output: a beat note with frequency f_{out} equal to the difference between the two lines.

Note that any effects of thermal and acoustic noise not suppressed by the common-mode rejection are attenuated by enclosing the cavity within three layers of thermal control and vibration isolation, illustrated by the

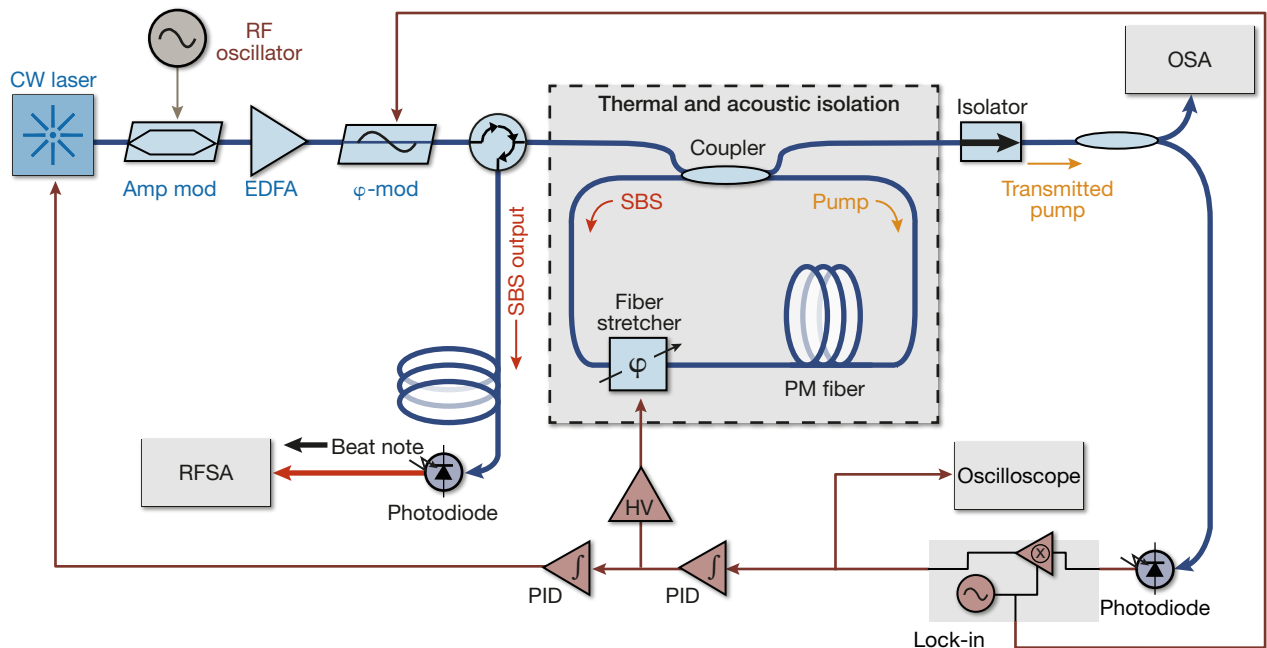


Figure 3. Experimental setup. Amp mod, amplitude modulator; CW, continuous wave; EDFA, erbium-doped fiber amplifier; HV, high-voltage amplifier; OSA, optical spectrum analyzer; PID, proportional–integral–differential amplifier; ϕ -mod, phase modulator; PM, polarization maintaining; RFSA, radio-frequency spectrum analyzer.

dashed box in Fig. 3. The synthesizer is further stabilized via two servo loops. The first servo is a high-bandwidth (≈ 2 -kHz) Pound–Drever–Hall loop⁴⁶ that uses a phase dither of ≈ 100 kHz and a lock-in amplifier to detect the positions of the pump lines with respect to the cavity resonances and to keep those resonances locked to the pump tones by tuning the cavity length via the fiber stretcher. The second loop is a much lower-bandwidth (< 100 -Hz) servo that integrates the correction signal from the first loop to drive the fine-tuning port of the master pump laser, thus tracking the pump laser to the cavity. With these nested servo loops in place, locking of the pump and cavity can be maintained over periods of hours.

Figure 4 is a photograph of the packaged SBS laser at the core of PFS. The rack-mountable chassis shown in the photo contains the elements shown inside the dashed box in Fig. 3 in addition to the circulator and isolator. On the left are a main power switch, a second toggle switch for disabling the central layer of heaters, and three temperature controllers, each of which is responsible for one layer of heaters. On the right are optical connectors for the pump input, transmitted pump output, and SBS lasing output, as well as an electrical connector for fiber-stretcher control voltage. An unused optical connector is also present so that an additional output can be easily added later.

PERFORMANCE

Optical Characterization

An optical spectrum of the pump and Stokes lines during operation at 8.350 GHz is shown in Fig. 5.



Figure 4. Photograph of the rack-mountable chassis containing the SBS laser.

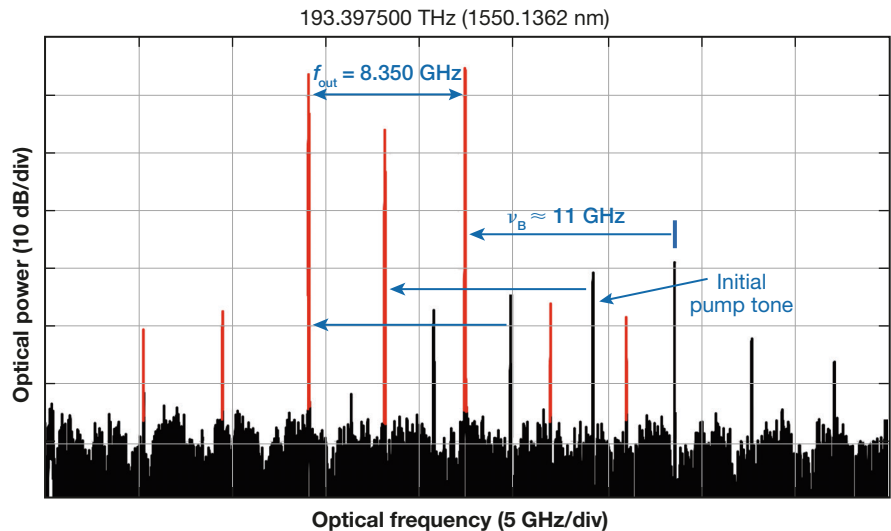


Figure 5. High-resolution optical spectrum of the optical pump and the Brillouin laser for a beat frequency of 8.350 GHz. The black trace shows the initial pump laser and its modulation sidebands. The red trace shows the SBS from the pump laser and its modulation sidebands. f_{out} , output frequency; ν_B , Brillouin shift.

The trace shown is a single spectrum; different components have been colored for illustrative purposes. The black components are the initial pump laser output at ν_0 (indicated by the arrow) and the modulation sidebands created by modulating at $f_0 = 4.175$ GHz. In this early experiment, a phase modulator was used for the f_0 modulation, resulting in numerous higher-order sidebands and substantial residual power at the original pump laser frequency. More recent experiments have used an intensity modulator, as diagramed in Fig. 3 and described above, which yields much weaker higher-order sidebands and minimal residual power at ν_0 . The red lines are SBS products, each of which is downshifted by ν_B from its pump. This experiment was conducted at an elevated temperature, so the Brillouin shift is 11.1 GHz.⁴⁷ Because there are seven pump lines (the initial pump, two first-order sidebands, two second-order sidebands, and two third-order sidebands), there are also seven SBS lines. Only the center three SBS lines are above the lasing threshold, and therefore they are substantially taller than the other red lines. The central pump tone was not suppressed, as noted above, so its SBS line is also above threshold. In our recent experiments this tone has been carefully minimized so no SBS lasing results from it.

Microwave Characterization and Tunability

Figure 6 shows the microwave spectrum of a 10.5-GHz beat note. The apparent linewidth in this trace is limited by the 3-Hz resolution of the spectrum analyzer. As will be discussed in the next subsection, we have shown the true instantaneous linewidth to be much less.

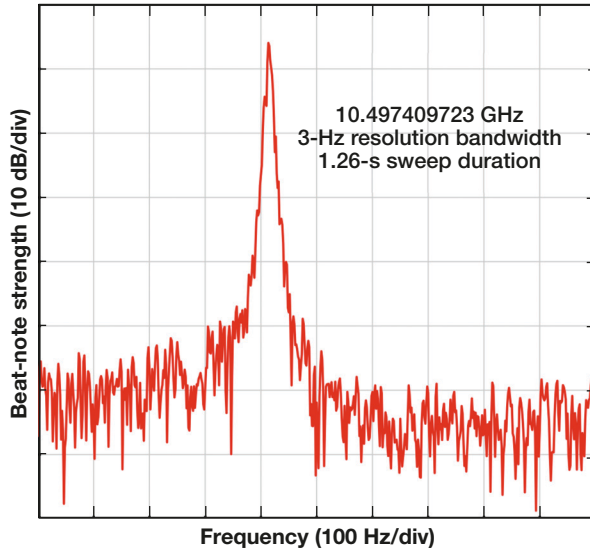


Figure 6. Microwave spectrum of the laser output at 10.5 GHz. Apparent linewidth is limited by the instrument resolution (3 Hz); actual RF linewidth is much less.

The description of the laser operation given above is valid for any combination of pump frequencies that places both pumps on resonances, so the beat note can be tuned in steps equal to the FSR. Figure 7 illustrates this tuning, showing every beat note from 10.45633 to 10.54900 GHz. Note that these frequencies are approximately 10 MHz apart, which agrees with the FSR estimated from the cavity length. Careful calculations indicate that the cavity FSR is $10,290,487 \pm 80$ Hz.²⁰ As Fig. 7 indicates, the beat-note spectra are essentially identical from one step to the next. The laser can be tuned over tens of thousands of FSRs. Figure 8 shows selected beat notes from 4.0 to 27.5 GHz, and we have tuned the laser both below¹⁷ and above²⁰ those frequencies.

The FSR itself is tunable over a very limited range. The intracavity phase shifter offers ~ 4 wavelengths of cavity-length tuning, yielding FSR tuning of approximately ± 2 Hz. Temperature tuning is also possible. The three-layer temperature regulation limits the thermal drift rate of the FSR to < 1 mHz/s, but the cavity temperature can be varied to enable slow tuning of a few hertz as well.

Figures 7 and 8 illustrate a key capability of the dual-wavelength laser as a PFS: Many individual frequencies, covering a broad frequency span, can be directly accessed simply by changing the pump wavelengths. For example, the current configuration can generate some 2300 evenly spaced frequencies over the span of Fig. 8. Furthermore, we have found that the performance, in terms of stability and noise, is consistent across this entire range. In a standard RF/microwave-frequency synthesizer, frequencies are generated via a combination of multiplication and mixing between multiple oscillators at fixed frequencies and/or tunable over a narrow frequency range. By using the dual-wavelength laser as a core element, a much simpler frequency synthesizer architecture can be envisioned wherein the gross frequency tuning is accomplished via the discrete tunability of the laser, with fine tuning via a single voltage-controlled oscillator, mixed in the RF domain with the nearest dual-wavelength laser frequency.

Noise, Linewidth, and Drift

Low-noise performance is critical for some of the most important applications of microwave oscillators, and the unique properties of this laser design yield exceptional

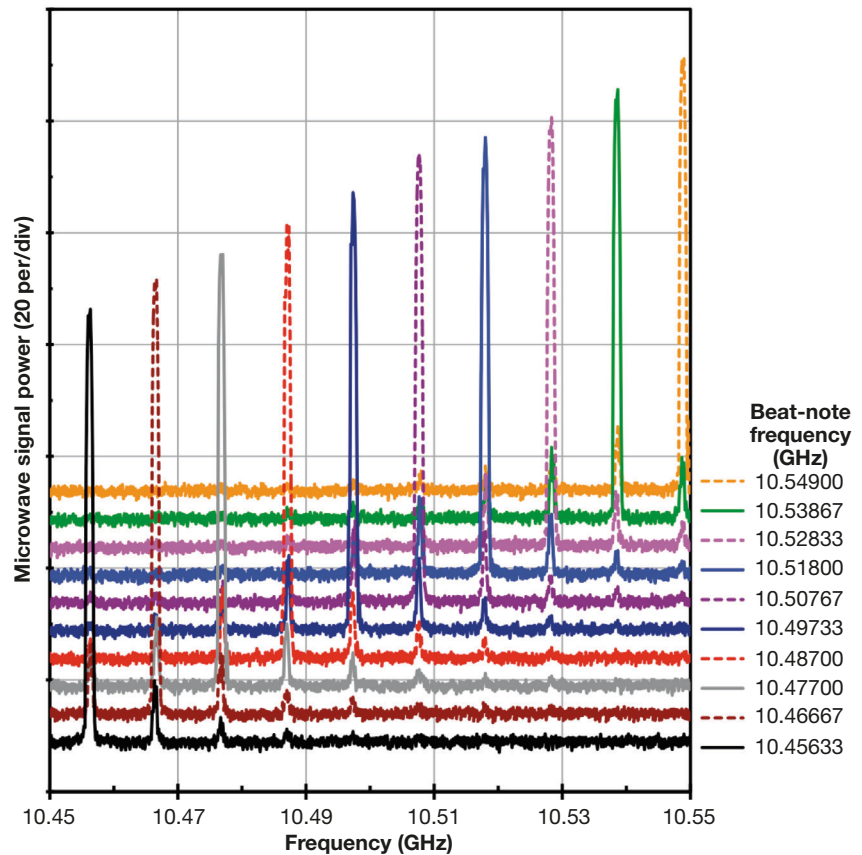


Figure 7. Ten RF spectra showing stepwise tunability of the PFS. The steps are equal to the FSR of the cavity ($10,290,487 \pm 80$ Hz).

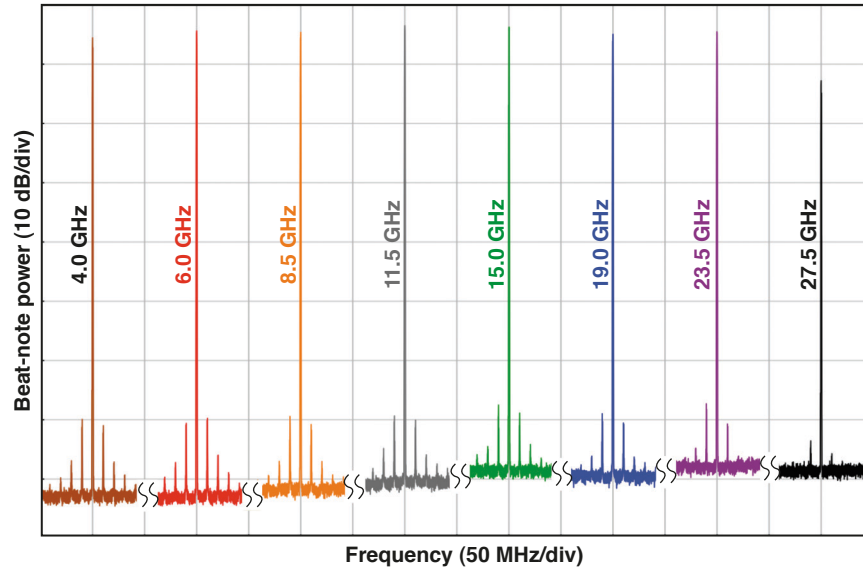


Figure 8. Microwave spectra showing operation at 4.0, 6.0, 8.5, 11.5, 15.0, 19.0, 23.5, and 27.5 GHz. Reduced power at 27.5 GHz is an artifact of the rolloff of the photodiode response. The PFS has been operated up to 100.0 GHz.

noise performance. Although the beat frequency f_{out} is very close to double the modulation frequency, the exact positions of the lasing lines and thus the exact value of the beat frequency are all determined by the positions of the cavity resonances, as illustrated in Fig. 2. As a result, the noise of the beat note is not strongly related to the noise on the modulation drive frequency. Rather, the noise is principally determined by the cavity resonances and, ultimately, by quantum noise of the lasing modes.

We characterized rejection of pump-frequency fluctuation by varying the pump separation (by tuning the modulation frequency) while recording the beat-note frequency and power. The results are plotted in Fig. 9. If the system simply replicated the pump-frequency noise, the beat-note frequency curve (blue) would have a slope of one. The slope is 0.0164, indicating that the system suppresses pump-frequency noise by a factor of 61.0 (17.9 dB). The beat-note power (red curve) is also relatively insensitive to pump-frequency variation. The full width at half maximum of this curve is

460 kHz, comparable to that of the cavity resonances, indicating that the resonances are the principal determinant of the beat-note frequency and power. We note that these results agree qualitatively with previous findings for single-wavelength SBS fiber lasers, namely that the transfer of the pump-frequency and pump-amplitude noise to the output is strongly suppressed.^{48–51}

Similarly, phase and frequency noise of the original pump laser do not affect the phase noise of the RF beat note. The key enabler of this feature is the cancellation of common-mode noise; most of the environmental noise that affects the optical frequencies $\nu_{1,out}$ and $\nu_{2,out}$ affects them in the same way, so that these noise effects cancel when the two frequencies

are differenced. The residual noise contributions from the cavity fluctuations can be determined beginning with the two optical frequencies given by Eq. 1,

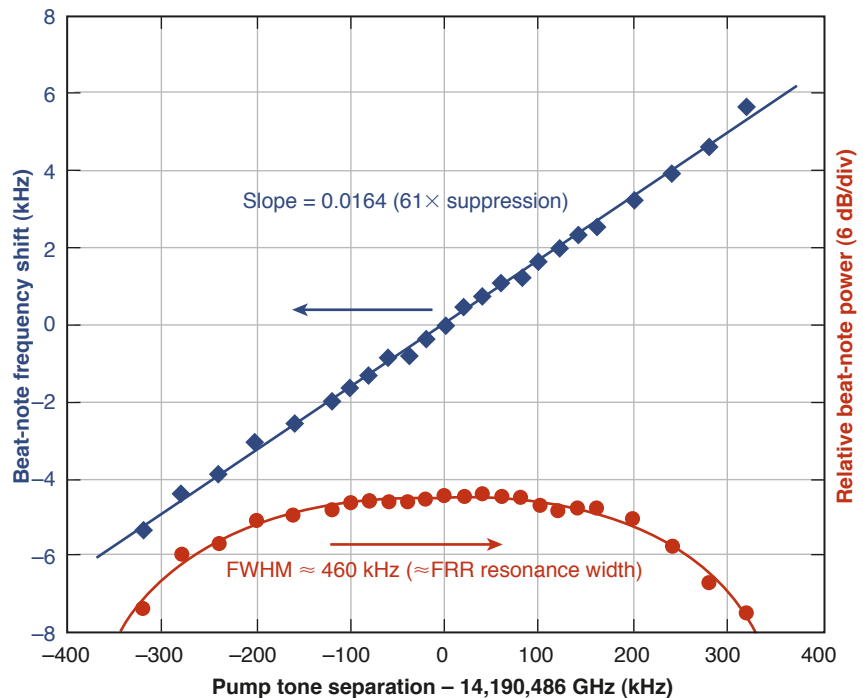


Figure 9. Two measurements illustrating the PFS's insensitivity to pump-frequency noise. The blue trace shows that the beat-note frequency suppresses noise on the RF drive frequency by a factor of 61. The red trace shows that beat-note power is weakly dependent on the input frequency over a range commensurate with the width of the cavity resonances. FWHM, full width at half maximum.

$$\begin{cases} \nu_{1,\text{out}} \\ \nu_{2,\text{out}} \end{cases} = \begin{cases} N_1 \Delta\nu_{\text{FSR}} \\ N_2 \Delta\nu_{\text{FSR}} \end{cases}, \quad (8)$$

where $N_{1,2}$ are (different) integers. The variation (noise) of each optical frequency due to fluctuations in the FRR is given by

$$\delta(\nu_{i,\text{out}}) = N_i \delta(\Delta\nu_{\text{FSR}}) = \frac{\nu_{i,\text{out}}}{\Delta\nu_{\text{FSR}}} \delta(\Delta\nu_{\text{FSR}}). \quad (9)$$

The absolute variation in the optical frequency can be significant, although it has been demonstrated that optical linewidths as narrow as 200 Hz can be obtained.^{15,52} Moreover, the noise on the optical frequencies due to variations in the FRR will be the same for both of the two optical frequencies; therefore, the noise on the beat frequency is

$$\begin{aligned} \delta f_{\text{out}} &= N_1 \delta(\Delta\nu_{\text{FSR}}) - N_2 \delta(\Delta\nu_{\text{FSR}}) \\ &= (N_1 - N_2) \delta(\Delta\nu_{\text{FSR}}). \end{aligned} \quad (10)$$

By substituting for the N_i from Eq. 8, and using Eq. 9, we can show that

$$\begin{aligned} \delta f_{\text{out}} &= \Delta\nu_{\text{RF}} \frac{\delta(\Delta\nu_{\text{FSR}})}{\Delta\nu_{\text{FSR}}} \\ &= \Delta\nu_{\text{RF}} \frac{\delta(\nu_{i,\text{out}})}{\nu_{i,\text{out}}}. \end{aligned} \quad (11)$$

Equation 11 illustrates that the residual fractional linewidth (i.e., $\delta f_{\text{out}}/f_{\text{out}}$) caused by cavity noise is equal to the fractional linewidth of the optical frequency mode. Using the 200-Hz optical linewidth mentioned above at an optical frequency of 193 THz (1550-nm wavelength) yields a fractional linewidth of $\sim 1 \times 10^{-12}$. For operation at 10 GHz, this implies a residual RF linewidth of 10 mHz would be obtained. Indeed, our recent precision phase noise measurements have yielded a linewidth of 3.2 mHz,⁵³ in rough agreement with this calculation.

Because the output frequency, f_{out} , is generated by the beating of two laser modes, the phase noise properties are ultimately limited by the phase noise characteristics—in the optical frequency domain—of the laser modes. The quantum-limited variance of the frequency is known as the Schawlow–Townes linewidth, $\Delta\nu_{\text{ST}}$, and is given by^{54,55}

$$\Delta\nu_{\text{ST}} = \frac{h\nu\theta\ell T_{\text{OC}}}{4\pi\tau_{\text{RT}}^2 P_{\text{out}}}, \quad (12)$$

where $h\nu$ is the photon energy, θ is a parameter referred to as the spontaneous emission factor (~ 500 for the cases to be considered here),⁵⁶ ℓ is the total round-trip cavity loss, T_{OC} is the output coupling from the resona-

tor, τ_{RT} is the round-trip transit time for the resonator, and P_{out} is the laser output power. The dual-sideband phase-noise spectrum corresponding to the linewidth of Eq. 12 was obtained in Ref. 55. The corresponding phase-noise spectrum, $S_{\phi}(f)$, expected for an electrical signal obtained by beating two quantum-limited laser modes together is

$$S_{\phi}(f) = \frac{\Delta\nu_{\text{ST}}}{\pi f^2}. \quad (13)$$

The phase noise of this synthesizer was characterized in Refs. 22 and 53. One key result is that the phase-noise spectrum is nearly independent of the beat-note frequency. This behavior contrasts starkly with traditional RF sources, in which the phase noise increases with increasing output frequency at a rate of 6 dB per octave. This result indicates that the phase noise is principally determined by the noise properties of the lasing modes and not technical noise sources in the resonator. For millimeter-wave frequencies, this SBS-based PFS is expected to offer phase-noise performance competitive with that of high-quality commercial oscillators; at even higher frequencies, the PFS is expected to offer superior noise performance.

APPLICATIONS AND FUTURE DIRECTIONS

In this article, we have discussed a Brillouin-laser-based photonic synthesizer of radio frequencies and microwaves. We have shown that this source is capable of producing discretely tunable frequencies up to tens of gigahertz. Potential military and commercial applications for a narrow-linewidth, low-noise synthesizer operating at demonstrated frequencies are manifold. A particular advantage of the PFS is that the laser output is already in optical fiber. The output can thus be transmitted over great distances with extremely low loss, using existing telecommunications technology, and then converted to an electrical signal directly at the site where the frequency is to be used. Our system is naturally suited to applications where it is advantageous to locate the master oscillator remotely from one or more user locations, such as time and frequency distribution⁵⁷ and remoting of communications or sensor antennas.⁵⁸

One commercial application we are actively pursuing is millimeter-wave fiber-radio communications.^{19,24} Frequencies in the range of 55–65 GHz offer the broad bandwidth required for high-data-rate links. This particular band is of interest for wideband personal-area networks because oxygen absorption in the atmosphere naturally limits the range. The limited range enables cellular network architectures with spatial frequency reuse analogous to current wireless networking standards in the 2.4-GHz band (e.g., Wi-Fi/IEEE 802.11),

but with vastly enhanced bandwidth. We have demonstrated data transport up to 3 Gb/s over distances up to ≈ 100 m, as described by Nanzer et al. elsewhere in this issue.

We believe that operation at much higher frequencies can be realized. In our current setup, the beat-note frequency is limited by the RF oscillator, the amplitude modulator, and the photodetector. We can eliminate the oscillator and the modulator by using two separate lasers to provide the two pump tones.¹⁶ These lasers can be arbitrarily far apart in frequency; at least one must be tunable in order to tune the beat note. The beat frequency from the SBS modes would be expected to have noise and stability properties comparable to what has been demonstrated in this work because of the common-cavity/common-mode noise-rejection mechanisms described above. With dual-laser pumping, the output frequency is limited only by the electrical bandwidth of the photodiode. Detector technology is advancing steadily, with 100-GHz photodiodes commercially available (e.g., from u²t Photonics AG of Berlin, Germany) and >300-GHz devices demonstrated.⁵⁹ These developments open up the prospect of using this technology for applications in the submillimeter-wave and terahertz-frequency regimes. Frequencies from 90 to 400 GHz are of interest for communications links, offering extremely high bandwidths for data-intensive applications such as multisensory telepresence and transmitting hyperspectral video. Certain frequency bands in the millimeter-wave regime can propagate through dust and other adverse atmospheric conditions; however, for commercially available power levels, range in the atmosphere is limited to 9000 m through clear air, depending on wavelength.⁶⁰ Rain and foliage reduce this range considerably. Frequencies in this range allow very small antennas, which are crucial for miniature UAVs and microsatellites. Atmospheric absorption is absent in outer space, so these frequency bands are especially compelling for high-bandwidth intersatellite cross-links.

Other potential applications for a PFS exist in research and development. One unique application is distribution of the master oscillator in millimeter-wave radio astronomy arrays. The Atacama Large Millimeter Array uses fiber-optic distribution of the master oscillator to coherently phase the receivers in the individual telescopes using a complex optical phase-locked loop.⁶¹ The PFS would have advantages over the current methods, including simpler construction, superior phase noise over a broad band of offset frequencies, and greater frequency flexibility. Additionally, the PFS offers benefits in the field of precision terahertz spectroscopy by extending the precision currently attainable at microwave frequencies into the terahertz regime.⁶²

High-precision applications, such as spectroscopy and navigation, would require long-term stabilization

to absolute physical references such as a molecular or atomic absorption line. Acetylene and cyanide standards exist in the ≈ 1550 -nm region where our system operates,^{63,64} and a technique for high-precision stabilization of a 1556-nm source to a ⁸⁵Rb reference has been demonstrated.⁶¹ Thus, this is a practical direction for future research. We are pursuing multiple approaches for attaining exceptionally low phase noise, with the objective of developing precision sources competitive with the best available microwave oscillators.⁶⁵

ACKNOWLEDGEMENTS: The research reported in this article was supported by internal research and development funding by the APL Air and Missile Defense Business Area.

REFERENCES

- ¹Lim, C., Nirmalathas, A., Bakaul, M., Lee, K.-L., Novak, D., and Waterhouse, R., "Mitigation Strategy for Transmission Impairments in Millimeter-Wave Radio-Over-Fiber Networks," *J. Opt. Netw.* **8**(2), 201–214 (2009).
- ²Gomes, N. J., Morant, M., Alphones, A., Cabon, B., Mitchell, J. E., et al., "Radio-Over-Fiber Transport for the Support of Wireless Broadband Services," *J. Opt. Netw.* **8**(2), 156–178 (2009).
- ³Stralka, J. P., and Fedarko, W. M., "Pulse Doppler Radar," in *Radar Handbook*, 3rd Ed., M. Skolnik (ed.), McGraw-Hill, New York, pp. 4.1–4.53 (2008).
- ⁴Williams, K. J., Goldberg, L., Esman, R. D., Dagenais, M., and Weller, J. F., "6–34 GHz Offset Phase-Locking of Nd:YAG 1319 nm Nonplanar Ring Lasers," *Electron. Lett.* **25**(18), 1242–1243 (1989).
- ⁵Simonis, G. J., and Purchase, D. G., "Optical Generation, Distribution, and Control of Microwaves Using Laser Heterodyne," *IEEE Trans. Microw. Theory Tech.* **38**(5), 667–669 (1990).
- ⁶Cliche, J.-F., Shillue, B., Têtu, M., and Poulin, M., "A 100-GHz-Tunable Photonic Millimeter Wave Synthesizer for the Atacama Large Millimeter Array Radiotelescope," in *IEEE/MTT-S International Microwave Symp.*, 2007, Honolulu, HI, pp. 349–352 (2007).
- ⁷Loh, W. H., de Sandro, J. P., Dowle, G. J., Samson, B. N., and Ellis, A. D., "40 GHz Optical-Millimetre Wave Generation with a Dual Polarization Distributed Feedback Fibre Laser," *Electron. Lett.* **33**(7), 594–595 (1997).
- ⁸Pajarola, S., Guekos, G., Nizzola, P., and Kawagucki, H., "Dual-Polarization External-Cavity Diode Laser Transmitter for Fiber-Optic Antenna Remote Feeding," *IEEE Trans. Microw. Theory Tech.* **47**(7), 1234–1240 (1999).
- ⁹Clark, T. R., Airola, M. G., and Sova, R. M., "Demonstration of Dual-Polarization Fiber Ring Laser for Microwave Generation," in *IEEE International Topical Meeting on Microwave Photonics*, 2004, Ogunquit, ME, pp. 127–130 (2004).
- ¹⁰Pillet, G., Morvan, L., Brunel, M., Bretenaker, F., Dolfi, D., et al., "Dual-Frequency Laser at 1.5 μm for Optical Distribution and Generation of High-Purity Microwave Signals," *J. Lightw. Tech.* **26**(15), 2764–2773 (2008).
- ¹¹Zhou, J. L., Xia, L., Cheng, X. P., Dong, X. P., and Shum, P., "Photonic Generation of Tunable Microwave Signals by Beating a Dual-Wavelength Single Longitudinal Mode Fiber Ring Laser," *Appl. Phys. B* **91**(1), 99–103 (2008).
- ¹²Pan, S. L., and Yao, J. P., "A Wavelength-Switchable Single-Longitudinal-Mode Dual-Wavelength Erbium-Doped Fiber Laser for Tunable Microwave Generation," *Opt. Express* **17**(7), 5414–5419 (2009).
- ¹³Demtröder, W., *Laser Spectroscopy: Basic Concepts and Instrumentation*, 3rd Ed., Springer, Berlin (2003).
- ¹⁴Siegman, A. E., *Lasers*, University Science Books, Mill Valley, CA, pp. 992–1003 (1986).

- ¹⁵Geng, J., Staines, S., Wang, Z., Zong, J., Blake, M., and Jiang, S., "Highly Stable Low-Noise Brillouin Fiber Laser with Ultranarrow Spectral Linewidth," *IEEE Photonics Technol. Lett.* **18**(17), 1813–1815 (2006).
- ¹⁶Geng, J. H., Staines, S., and Jiang, S. B., "Dual-Frequency Brillouin Fiber Laser for Optical Generation of Tunable Low-Noise Radio Frequency/Microwave Frequency," *Opt. Lett.* **33**(1), 16–18 (2008).
- ¹⁷Dennis, M. L., Sova, R. M., and Clark, T. R., "Dual-Wavelength Brillouin Fiber Laser for Microwave Frequency Generation," in *Conf. on Optical Fiber Communication and the National Fiber Optic Engineers Conf.*, 2007, Anaheim, CA, paper OWJ6 (2007).
- ¹⁸Dennis, M. L., Sova, R. M., and Clark, T. R., "Microwave Frequency Generation up to 27.5 GHz Using a Dual-Wavelength Brillouin Fiber Laser," in *2007 Digest of the IEEE/LEOS Summer Topical Meetings*, Portland, OR, pp. 194–195 (2007).
- ¹⁹Dennis, M. L., Gross, M. C., Clark, T. R., Novak, D., and Waterhouse, R. B., "Broadband Data Transmission in a 40 GHz Fiber Radio Link Using a Dual-Wavelength SBS Fiber Laser," in *Conf. on Optical Fiber Communication and the National Fiber Optic Engineers Conf.*, San Diego, CA, paper OWF4 (2009).
- ²⁰Gross, M. C., Callahan, P. T., Clark, T. R., Novak, D., Waterhouse, R. B., and Dennis, M. L., "Tunable Millimeter-Wave Frequency Synthesis Up to 100 GHz by Dual-Wavelength Brillouin Fiber Laser," *Opt. Express* **18**(13), 13321–13330 (2010).
- ²¹Gross, M. C., Clark, T. R., and Dennis, M. L., "Narrow-Linewidth Microwave Frequency Generation by Dual-Wavelength Brillouin Fiber Laser," in *21st Annual Meeting of the IEEE Lasers and Electro-Optics Society, 2008 (LEOS 2008)*, Newport Beach, CA, pp. 151–152 (2008).
- ²²Callahan, P. T., Gross, M. C., and Dennis, M. L., "Phase Noise Measurements of a Dual-Wavelength Brillouin Fiber Laser," in *2010 IEEE Topical Meeting on Microwave Photonics (MWP)*, Montreal, QC, Canada, pp. 155–158 (2010).
- ²³Dennis, M. L., Callahan, P. T., and Gross, M. C., "Suppression of Relative Intensity Noise in a Brillouin Fiber Laser by Operation Above Second-Order Threshold," in *23rd Annual Meeting of the IEEE Photonics Society, 2010*, Denver, CO, pp. 28–29 (2010).
- ²⁴Dennis, M. L., Nanzer, J. A., Callahan, P. T., Gross, M. C., Clark, T. R., et al., "Photonic Upconversion of 60 GHz IEEE 803.15.3c Standard Compatible Data Signals Using a Dual-Wavelength Laser," in *23rd Annual Meeting of the IEEE Photonics Society, 2010*, Denver, CO, pp. 383–384 (2010).
- ²⁵Stokes, L. F., Chodorow, M., and Shaw, H. J., "All-Single Mode Fiber Resonator," *Opt. Lett.* **7**(6), 288–290 (1982).
- ²⁶Meyer, R. E., Ezekiel, S., Stowe, D. W., and Tekippe, V. J., "Passive Fiber-Optic Ring Resonator for Rotation Sensing," *Opt. Lett.* **8**(12), 644–646 (1983).
- ²⁷Hotate, K., "Fiber Sensor Technology Today," *Opt. Fiber Technol.* **3**(4), 356–402 (1997).
- ²⁸Yue, C. Y., Peng, J. D., Liao, Y. B., and Zhou, B. K., "Fiber Ring Resonator with Finesse of 1260," *Electron. Lett.* **24**(10), 622–623 (1988).
- ²⁹Tai, S., Kyuma, K., Hamanaka, K., and Nakayama, T., "Applications of Fibre Optic Ring Resonators Using Laser Diodes," *Optica Acta* **33**(12), 1539–1551 (1986).
- ³⁰Kalli, K., and Jackson, D. A., "Ring Resonator Optical Spectrum Analyzer with 20-kHz Resolution," *Opt. Lett.* **17**(15), 1090–1092 (1992).
- ³¹Agrawal, G. P., *Nonlinear Fiber Optics*, 2nd Ed., Academic Press, San Diego (1995).
- ³²Niklès, M., Thévenaz, L., and Robert, P. A., "Brillouin Gain Spectrum Characterization in Single-Mode Optical Fibers," *J. Lightw. Technol.* **15**(10), 1842–1851 (1997).
- ³³Hill, K. O., Kawasaki, B. S., and Johnson, D. C., "CW Brillouin Laser," *Appl. Phys. Lett.* **28**(10), 608–609 (1976).
- ³⁴Ponikvar, D. R., and Ezekiel, S., "Stabilized Single-Frequency Stimulated Brillouin Fiber Ring Laser," *Opt. Lett.* **6**(8), 398–400 (1981).
- ³⁵Stokes, L. F., Chodorow, M., and Shaw, H. J., "All-Fiber Stimulated Brillouin Ring Laser with Submilliwatt Pump Threshold," *Opt. Lett.* **7**(10), 509–511 (1982).
- ³⁶Smith, D. W., Cotter, D., and Wyatt, R., "Method and Apparatus for Generating Coherent Radiation," U.S. Patent 4,780,876 (25 Oct 1988).
- ³⁷Smith, S. P., Zarinetchi, F., and Ezekiel, S., "Narrow Linewidth Stimulated Brillouin Fiber Laser and Applications," *Opt. Lett.* **16**(6), 393–395 (1991).
- ³⁸Thomas, P. J., van Driel, H. M., and Stegeman, G. I. A., "Possibility of Using an Optical Fiber Brillouin Ring Laser for Inertial Sensing," *Appl. Opt.* **19**(12), 1906–1908 (1980).
- ³⁹Vali, V., and Shorthill, R. W., "Stimulated Brillouin Scattering Ring Laser Gyroscope," U.S. Patent 4,159,178 (26 June 1979).
- ⁴⁰Kadiwar, R. K., and Giles, I. P., "Optical Fibre Brillouin Ring Laser Gyroscope," *Electron. Lett.* **25**(25), 1729–1731 (1989).
- ⁴¹Dyes, W. A., and Farhad, H., "Scattered Light Multi-Brillouin Gyroscope," U.S. Patent 5,064,288 (12 Nov 1991).
- ⁴²Zarinetchi, F., Smith, S. P., and Ezekiel, S., "Stimulated Brillouin Fiber-Optic Gyroscope," *Opt. Lett.* **16**(4), 229–231 (1991).
- ⁴³Quast, T., and Raab, M., "Brillouin Ring Laser," U.S. Patent 5,323,415 (21 June 1994).
- ⁴⁴Raab, M., "Brillouin Ring Laser Gyro," U.S. Patent 5,517,305 (14 May 1996).
- ⁴⁵Wooten, E. L., Kissa, K. M., Yi-Yan, A., Murphy, E. J., Lafaw, D. A., et al., "A Review of Lithium Niobate Modulators for Fiber-Optic Communications Systems," *IEEE J. Sel. Top. Quantum Electron.* **6**(1), 69–82 (2000).
- ⁴⁶Black, E. D., "An Introduction to Pound-Drever-Hall Laser Frequency Stabilization," *Am. J. Phys.* **69**(1), 79–87 (2001).
- ⁴⁷Yu, Q., Bao, X., and Chen, L., "Temperature Dependence of Brillouin Frequency, Power, and Bandwidth in Panda, Bow-Tie, and Tiger Polarization-Maintaining Fibers," *Opt. Lett.* **29**(1), 17–19 (2004).
- ⁴⁸Debut, A., Randoux, S., and Zemmouri, J., "Linewidth Narrowing in Brillouin Lasers: Theoretical Analysis," *Phys. Rev. A* **62**(2), 023803-1–023803-4 (2000).
- ⁴⁹Debut, A., Randoux, S., and Zemmouri, J., "Experimental and Theoretical Study of Linewidth Narrowing in Brillouin Fiber Ring Lasers," *J. Opt. Soc. Am. B* **18**(4), 556–567 (2001).
- ⁵⁰Stépien, L., Randoux, S., and Zemmouri, J., "Intensity Noise in Brillouin Fiber Ring Lasers," *J. Opt. Soc. Am. B* **19**(5), 1055–1066 (2002).
- ⁵¹Molin, S., Baili, G., Alouini, M., Dolfi, D., and Huignard, J.-P., "Experimental Investigation of Relative Intensity Noise in Brillouin Fiber Ring Lasers for Microwave Photonics Applications," *Opt. Lett.* **33**(15), 1681–1683 (2008).
- ⁵²Geng, J., Staines, S., Wang, Z., Zong, J., Blake, M., and Jiang, S., "Actively Stabilized Brillouin Fiber Laser with High Output Power and Low Noise," in *Optical Fiber Communication Conf., 2006 and the 2006 National Fiber Optic Engineers Conf. (OFC 2006)*, Anaheim, CA, paper OThC4 (2006).
- ⁵³Callahan, P. T., Gross, M. C., and Dennis, M. L., "Frequency-Independent Phase Noise of a Dual-Wavelength Brillouin Fiber Laser," *IEEE J. Quantum Electron.* (in press).
- ⁵⁴Schawlow, A. L., and Townes, C. H., "Infrared and Optical Masers," *Phys. Rev.* **112**(6), 1940–1949 (1958).
- ⁵⁵Paschotta, R., Schlatter, A., Zeller, S. C., Telle, H. R., and Keller, U., "Optical Phase Noise and Carrier-Envelope Offset Noise of Mode-Locked Lasers," *Appl. Phys. B* **82**(2), 265–273 (2006).
- ⁵⁶Olsson, N. A., and Van Der Ziel, J. P., "Characteristics of a Semiconductor Laser Pumped Brillouin Amplifier with Electronically Controlled Bandwidth," *J. Lightw. Technol.* **LT-5**(1), 147–153 (1987).
- ⁵⁷Ye, J., Peng, J.-L., Jones, R. J., Holman, K. W., Hall, J. L., et al., "Delivery of High-Stability Optical and Microwave Frequency Standards over an Optical Fiber Network," *J. Opt. Soc. Am. B* **20**(7), 1459–1467 (2003).
- ⁵⁸Seeds, A. J., "Microwave Photonics," *IEEE Trans. Microw. Theory Tech.* **50**(3), 877–887 (2002).
- ⁵⁹Beling, A., and Campbell, J. C., "InP-Based High-Speed Photodetectors," *J. Lightw. Technol.* **27**(3), 343–355 (2009).
- ⁶⁰Marcus, M., and Pattan, B., "Millimeter Wave Propagation: Spectrum Management Implications," *IEEE Microw. Mag.* **6**(2), 54–62 (2005).
- ⁶¹Cliche, J.-F., Shillue, B., Latrasse, C., Tétu, M., and D'Addario, L., "A High Coherence, High Stability Laser for the Photonic Local Oscillator Distribution of the Atacama Large Millimeter Array," in *Ground-based Telescopes*, Proc. SPIE, Vol. 5489, J. M. Oschmann Jr. (ed.), SPIE, Bellingham, WA, pp. 1115–1126 (2004).

⁶²De Lucia, F. F., "Spectroscopy in the Terahertz Spectral Region," in *Sensing with Terahertz Radiation*, D. Mittleman (ed.), Springer, Berlin (2003).

⁶³Gilbert, S. L., and Swann, W. C., *Acetylene $^{12}\text{C}_2\text{H}_2$ Absorption Reference for 1510 nm to 1540 nm Wavelength Calibration—SRM 2517a*, National Institute of Standards and Technology Special Publication 260-133, 2001 Ed., U.S. Government Printing Office, Washington, DC (2001).

⁶⁴Gilbert, S. L., Swann, W. C., and Wang, C. M., *Hydrogen Cyanide $\text{H}^{13}\text{C}^{14}\text{N}$ Absorption Reference for 1530–1560 nm Wavelength Calibration—SRM 2519*, National Institute of Standards and Technology Special Publication 260-137, U.S. Government Printing Office, Washington, DC (1998).

⁶⁵Ivanov, E. N., and Tobar, M. E., "Low Phase-Noise Sapphire Crystal Microwave Oscillators: Current Status," *IEEE Trans. Ultrason. Ferroelectr. Freq. Control.* **56**(2), 263–269 (2009).

The Authors



Michael C.
Gross



Patrick T.
Callahan



Michael L.
Dennis

Michael C. Gross is a member of the Senior Professional Staff in APL's Research and Exploratory Development Department. Dr. Gross was responsible for assembling the synthesizer and its environmental control, and he was instrumental in extending the system's capabilities to millimeter-wave frequencies. **Patrick T. Callahan** was previously a member of the Associate Professional Staff in the Electro-Optical and Infrared Systems and

Technology Group in APL's Air and Missile Defense Department and is now with the Department of Electrical Engineering and Computer Science at the Massachusetts Institute of Technology. Mr. Callahan carried out extensive characterization of the synthesizer's noise properties and was invaluable in the application of the system to high-frequency carrier and waveform synthesis and to millimeter-wave communications. **Michael L. Dennis** is a Principal Professional Staff member in the Air and Missile Defense Department and the Principal Investigator on this project. Dr. Dennis invented the dual-mode Brillouin synthesizer, constructed and tested the first prototype system, and was extensively involved in the work described here as well as in developing potential applications. For further information on the work reported here, contact Michael Gross. His e-mail address is michael.gross@jhuapl.edu.